monoclonal antibody (Fig. 3*d*). The amino-acid sequence analysis (up to residue 14) was identical to that for the mouse. Thus, cachexia in mice and humans appears to be associated with the same material.

These data suggest that the 24K proteoglycan represents a potential mediator of the process of cancer cachexia. It is distinguished from the cytokines, not only in structure, but by the ability to accelerate breakdown of skeletal muscle *in vitro* and *in vivo* and to produce weight loss *in vivo* by a process not involving anorexia. Thus this material may induce the metabolic component of cachexia, because the cytokines are invariably associated with anorexia. The 24K proteoglycan shows a strong association with the development of clinical cancer cachexia, because immunoreactive material is detectable in the urine of all patients so far investigated who are actively losing weight, irrespective of tumour type. This suggests that this material may play an active role in the development of human cancer cachexia. □

Received 24 October 1995; accepted 5 January 1996.

1. Beutler, B & Cerami, A. *Nature* **320,** 584–588 (1986).
2. Strassman, G., Fong, M., Kenney, J. S. & Jacob, C. O. *J. clin. Invest.* **89,** 1681–1684 (1992).
3. Matthys, P. *et al. Int. J. Cancer* **49,** 77–82 (1991).
4. Mori, M. *et al. Cancer Res.* **51,** 6656–6659 (1991).
5. Socher, S. H., Martinez, D., Craig, J. B., Kuhn, J. K. & Oliff, A. *J. natl. Cancer Inst.* **80,** 595–598 (1988).
6. Soda, K., Kawakami, M., Kashii, A. & Miyata, M. *Jap. J. Cancer Res.* **85,** 1124–1130 (1994).
7. Metcalf, D., Nicola, N. A. & Gearing, D. P. *Blood* **76,** 50–56 (1990).
8. Bibby, M. C. *et al. J. natn. Cancer Inst.* **78,** 539–546 (1987).
9. Beck, S. A. & Tisdale, M. J. *Cancer Res.* **47,** 5919–5923 (1987).
10. McDevitt, T. M., Todorov, P. T., Beck, S. A., Khan, S. H. & Tisdale, M. J. *Cancer Res.* **55,** 1458–1463 (1995).
11. Yoshizawa, N., Oshima, S., Sagel, I., Shimizu, J. & Treser, G. *J. Immun.* **148,** 3110–3116 (1992).
12. Plumb, J. A., Fearon, K. C. H., Carter, K. B. & Preston, T. *Clin. Nutr.* **10,** 23–29 (1991).
13. Smith, K. L. & Tisdale, M. J. *Br. J. Cancer* **68,** 314–318 (1993).
14. McDevitt, T. M. & Tisdale, M. J. *Br. J. Cancer* **66,** 815–820 (1992).
15. Goldberg, A., Kettlehut, K., Fagan, J. & Baracos, V. *J. clin. Invest.* **81,** 1378–1383 (1988).
16. Garcia-Martinez, C., Lopez-Soriano, F. J. & Argiles, J. M. *Cancer Lett.* **76,** 1–4 (1994).
17. Beck, S. A., Smith, K. L. & Tisdale, M. J. *Cancer Res.* **51,** 6089–6093 (1991).

ACKNOWLEDGEMENTS. We thank S. Wigmore, Department of Surgery, Edinburgh Royal Infirmary and K. Alpar, Department of Surgery, Selly Oak Hospital, Birmingham for providing the patient urine samples. This work was supported by a grant from the Cancer Research Campaign.

Inhibition of G-protein-mediated MAP kinase activation by a new mammalian gene family

Kirk M. Druey, Kendall J. Blumer, Veronica H. Kang & John H. Kehrl*

Laboratory of Immunoregulation, National Institute of Allergy and Infectious Diseases, National Institutes of Health, Bethesda, Maryland 20892-1876, USA, and Department of Cell Biology and Physiology, Washington University School of Medicine, St Louis, Missouri 63110, USA

A GENERAL property of signal transduction pathways is that prolonged stimulation decreases responsiveness, a phenomenon termed desensitization. Yeast cells stimulated with mating pheromone activate a heterotrimeric G-protein-linked, MAP-kinase-dependent signalling pathway that induces G1-phase cell-cycle arrest and morphological differentiation (reviewed in refs 1, 2). Eventually the cells desensitize to pheromone and resume growth[3]. Genetic studies have demonstrated the relative importance of a desensitization mechanism that uses the *SST2* gene product, Sst2p[4–7]. Here we identify a mammalian gene family termed *RGS* (for regulator of G-protein signalling) that encodes structural and functional homologues of Sst2p. Introduction of *RGS* family members into yeast blunts signal transduction through the pheromone-response pathway. Like *SST2* (refs 8–10), they negatively regulate this pathway at a point upstream or at the level of the G protein. The RGS family members also markedly impair MAP kinase activation by mammalian G-protein-linked receptors, indicating the existence and importance of an *SST2*-like desensitization mechanism in mammalian cells.

Although close homologues of Sst2p have not been reported, we studied an expanding family of mammalian genes that encodes proteins with a conserved domain (RGS domain) related to a region in Sst2p. It is even more closely to a region in flbA, a protein encoded by an *SST2*-related gene in *Aspergillus nidulans*[11]. The first *RGS* family member, *BL34* (*RGS1*), was found during screens for B-lymphocyte-specific genes and activation genes in chronic lymphocytic leukaemia cells[12,13]. A search for activation genes in peripheral blood mononuclear cells, which led to the isolation of *GOS8* (ref. 14), provided evidence that *RGS1* belongs to a gene family. The predicted G0S8 (RGS2) and RGS1 proteins have similar relative molecular mass and 42% amino-acid identity. In addition, an evolutionarily conserved homologue was found in *Caenorhabditis elegans*[15].

A Southern blot, using human genomic DNA hybridized with an oligonucleotide that was based on a highly conserved portion of the RGS domain, predicted a minimum of 15 family members (data not shown). A screen of a B-cell complementary DNA library with the same probe identified a new *RGS* family member, *RGS3*, which encodes a protein of 519 amino acids and has a relative molecular mass of 57,000 (M_r 57K) (Fig. 1*a*,*b*). An acidic region (residues 181–226), predicted to assume a coiled-coil[16], is located outside the region homologous to RGS1 and RGS2. To the amino-terminal side of the coiled-coil is a region rich in proline and glutamine that contains a hexapeptide repeat of the motif (Q, K)(D, E)(P, L)(P, L)(P, X)X and overlaps four PEST sequences (amino acids 30–46, 48–64, 66–82 and 84–111). Northern blot analysis (Fig. 1*c*) indicated that there are two major RSG3 transcripts present in multiple tissues.

The identification of a fourth *RGS* family member in a screen of rat brain cDNAs, the expression of which allowed *sst2*Δ mutants to grow on pheromone-containing plates, provided the first direct evidence of a functional significance of the sequence homologies noted between the *RGS* family members and *SST2*. *RGS4* encodes a protein of 205 amino acids, 37% identical to RGS1 (Fig. 2*a*). A TFASTA database search identified a partial cDNA sequence (GBN:HSC1YC111, accession number F07191) for the human orthologue, and a human *RGS4* cDNA (the protein of which has 97% amino acid identity with rat RGS4) was isolated. Further database searches identified three other putative RGS family members: one from infant brain and lung (accession numbers D311257 and R35272); a second from fetal lung and infant brain (accession numbers H09621 and L40394); and a third from adult lung (accession number T94013). These three genes were designated *RGS5*, *RGS6* and *RGS13*, respectively (Fig. 2*b*). Northern blot analysis identified *RGS4* transcripts only in brain (Fig. 2*c*).

To determine whether other *RGS* family members function in yeast, we introduced expression plasmids for *RGS1*, *RGS2*, *RGS3* and *RGS4*, as well as a truncation of *RGS3* (*RGS3T*) that retains the coding region for the RGS domain (residues 314–519), into an *sst2*Δ strain. Their expression partially complemented the pheromone-supersensitive phenotype of the *sst2*Δ mutant, as judged by growth-arrest (halo) assays. Dose–response relationships indicated that they reduced pheromone sensitivity as follows: *RGS4*, >30-fold; *RGS1* and *RGS3T*, 10–30-fold; *RGS3* and *RGS2*, 3-fold (Fig. 3*a*). Furthermore, their expression in wild-type cells decreased pheromone sensitivity, as indicated by the formation of turbid zones of growth inhibition (Fig. 3*b*), and expression of *RGS4* in the *sst2*Δ mutant partly blocked pheromone-induced expression of a reporter gene, both in terms of apparent EC_{50} (the effector concentration for half-maximum response) and maximal level of expression (Fig. 3*c*).

We used genetic tests to determine where in the pheromone response pathway the RGS family members function. As judged by assays of G1 arrest and transcriptional responses, neither *RGS4*

* To whom correspondence should be addressed.

a

```
MFETEADEKREMALEEGKGPGAEDSPPSKEPSPGQELPPGQD     42
LPPNKDSPSGQEPAPSQEPLSSKDSATSEGSPPGPDAPPSKD     84
VPPCQEPPPAQDLSPCQDLPAGQEPLPHQDPLLTKDLPAIQE    126
SPTRDLPPCQDLPPSQVSLPAKALTEDTMSSGDLLAATGDPP    168
AAPRPAFVIPEVRLDSTYSQKAGAEQGCSGDEEDAEEAEEVE    210
EGEEGEEDEDEDTSDDNYGERSEAKRSSMIETGQGAEGGLSL    252
RVQNSLRRRTHSEGSLLQEPRGPCFASDTTLHCSDGEGAAST    294
WGMPSPSTLKKELGRNGGSMHHLSLFFTGHRKMSGADTVGDD    336
DEASRKRKSKNLAKDMKNKKGIFRRRNESPGAPPAGKADKMM    378
KSFKPTSEEALKWGESLEKLLVHKYGLAVFQAFLRTEFSEEN    420
LEFWLACEDFKKVKSQSKMASKAKKIFAEYIAIQACKEVNLD    462
SYTREHTKDNLQSVTRGCFDLAQKRIFGLMEKDSYPRFLRSD    504
LYLDLINQKKMSPPL                               519
```

b

```
RGS3   330  ADTVGDDDEASRKRKSKNLAKDMKNKLGIFRRRNESPGAPPA  371
RGS1    15  GTTHSLLDDKMQKRRPKTFGMDMKA----YLRSMIPHLESGM   51
RGS2    19  SAGSGHKSEEKREKMKRTLLKDWKTRLSYFLQNSSTPGKPKT   60
                          * *

RGS3   372  -GKADKMMKSFKPTSEEALKWGESLEKLLVHKYGLAVFQAFL  412
RGS1    52  KSSKSKDV----LSAAEVMQWSQSLEKLLANQTGQNVFGSFL   90
RGS2    61  -GKKSKQQAFIKPSPEEAQLWSEAFDELLASKYGLAAFRAFL  101
                *          *   *      **    *  *  **

RGS3   413  RTEFSEENIEFWLACEDFKKVKSQSKMASKAKKIFAEYIAIQ  454
RGS1    91  KSEFSEENIEFWLACEDYKKTES-DLLPCKAEEIYKAFVHSD  131
RGS2   102  KSEFCEENIEFWLACEDFKKTKSPQKLSSKARKIYTDFIEKE  143
              ** ************ **  *      **  *

RGS3   455  ACKEVNLDSYTREHTKDNLQSVTRGCFDLAQKRIFGLMEKDS  496
RGS1   132  AAKQINIDFRTRESTAKKIKAPTPTCFDEAQKVIYTLMEKDS  173
RGS2   144  APKEINIDFQTKTLIAQNIQEATSGCFTTAQKRVYSLMENNS  185
            * *  * *  *           *  **    **    ***  *

RGS3   497  YPRFLRSDLYLDLINQKKMSP   517
RGS1   174  YPRFLKSDIYLNLLNDLQANS   194
RGS2   185  YPRFLESEFYQDLCKKPQITT   106
            ***** *  *  *
```

c

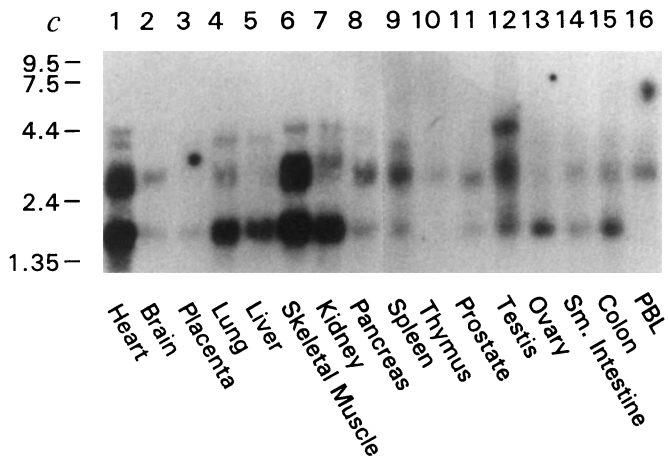

FIG. 1 Isolation and characterization of a new RGS family member. *a*, Amino-acid sequence of RGS3. The first 5 amino acids of the hexapeptide repeats and the acidic region are underlined. *b*, Alignment of RGS1, RGS2 and RGS3. The RGS domain of the various family members is indicated. *c*, Northern blot analysis of 2 μg poly(A) RNA prepared from multiple tissues hybridized with a full-length *RGS3* cDNA insert.

METHODS. An oligonucleotide probe (5′-GAG GAG AAT ATT GAG TTC TGG CTG GCT TGT GAA GAC T-3′) derived from a highly conserved region between *RGS1* and *RGS2* was used to isolate *RGS3* from a human tonsil B-cell cDNA library. The derived nucleotide sequence from the *RGS3* cDNA was compared with the GenBank Genetic Sequence Data Bank at the Frederick Biomedical Supercomputing Center.

a

```
MCKGLAGLPASCLRSAKDMKHRLGFLLQKSDSCEH     35
SSSHSKKDKVVTCQRVSQEEVKKWAESLENLINHE     70
CGLAAFLAFLKSEYSEENIDFWISCEEYKKIKSPS    105
KLSPKAKKIYNEFISVQATKEVNLDSCTREETSRN    140
MLEPTITCFDEAQKKIFNLMEKDSYRRFLKSRFYL    175
DLTNPSSCGAEKQKGAKSSADCTSLVPQCA
```

FIG. 2 Characterization of RGS4 and alignment of various RGSs. *a*, Amino-acid sequence of RGS4. The RGS domain is underlined. *b*, Alignment of the RGS family members to corresponding regions in flbA and Sst2p and *C. elegans* C05B5.7. The RGS5, RGS6 and RGS13 sequences are incomplete over the entire region spanned by the RGS domain. The nomenclature for the *RGS* family members was developed in conjunction with M. Koelle (ref. 22), resulting in the numbering of the seventh member, which we identified, as *RGS13*. Gaps of 93 and 27 amino acids in the Sst2p and flbA sequences, respectively, were introduced in the alignment. *c*, *RGS4* mRNA expression in various tissues. Northern blot analysis of 2 μg poly(A) RNA prepared from multiple human tissues (lanes 1–8) and portions of the brain (lanes 9–16) hybridized with the full-length human *RGS4* cDNA insert. The autoradiographs were exposed overnight.

METHODS. A rat brain cDNA library in the yeast high-copy expression vector pVT102U was used to isolate *RGS4*. Five pools of the library were transformed into an *sst2Δ* mutant (BC180) and plated directly onto selective media containing 10 nM α-factor. Pheromone-resistant colonies were tested for mating ability, and non-maters discarded. The remaining clones were analysed by pheromone-induced growth arrest (halo) assays. We isolated 12 plasmids, six with identical restriction maps, and the nucleotide sequence of one (pVT102U–*RGS4*) was determined. The human *RGS4* cDNA was isolated from a brain cDNA library (Clontech) by the polymerase chain reaction (PCR) and its nucleotide sequence determined.

b

```
RGS1    KWGESLEKLLVHKYGLAVFQAFLRTEFSEENIEFWLACEDYKKTESDLLPCKAEEIYKAF   127
RGS2    LWSEAFDELLASKYGLAAFRAFLKSEFCEENIEFWLACEDFKKTKSPQKLSSKARKIYTD   138
RGS3    KWGESLEKLLVHKYGLAVFQAFLRTEFSEENIEFWLACEDFKKVKSQSKMASKAKKIFAE   449
RGS4    KWAESLENLINHECGLAAFLAFLKSEYSEENIDFWISCEEYKKIKSPSKLSPKAKKIYNE   117
RGS5    QWRDSLDKLLQNNYGLASFKSFLKSEFSEENLEFWIACEDYKKIKSPAKMAEKAKQIYEE   132
RGS13   QWAQSFENLMATKYGPVVYAAYLKMEHSDENIQFWMACETYKKIASRWSRISRAKXLYKI    88
C05B5.7 SWQQSFDTLMSFKSGQKCFAEFLKSEYSDENILFWQACEELKREKNSEKMEEKARIIYED    93
FLBA    SNNARLNHILQDPALRLLFREFLRFSLCEENLSFYIDVSEFTTQYHKFDKVGHFKKPDAV   598
SST2    SNLNKLDYVLTDPGMRYLFRRHLEKELCVENLDVFIEIKRFLKKMTILKKLIDSKHCDKK   475
consensus       **        *  *L  * * EN*  * **   **

RGS1    -VHSDAKKQINIDFRTRESTAKKIKAPTPTCFDEAQKVIYTLMEKDSYPRFLKSDIYLNL   186
RGS2    FIEKEAPKEINIDFQTKTLIAQNIQEATSGCFTTAQKRVYSLMENNSYPRFLESEFYQDL   198
RGS3    YIAIQACKEVNLDSYTREHTKDNLQSVTRGCFDLAQKRIFGLMEKDSYPRFLRSDLYLDL   509
RGS4    FISVQATKEVNLDSCTREETDRNMLEPTITCFDEAQKKIFNLMEKDSYRRFLKSRFYLDL   177
RGS5    FIQTEAPKEVNIDHFTKDITMKNLVEPSLSSFDMAQKRIHALMEKDSLPRFVRSEFYQEL   192
RGS6    FLAPGAPSAINLDSHSYEITSQNVKDGGRYTFEDAQEHIYKLMKSDSYARFPPVKCLPGF    90
C05B5.7 FISILSPKEVSLDSKVREIVNTNMSRPTQNTFEDAQHQIYQLMARDSYPRFLTSIFYRET   123
FLBA    ALRNSLASRMTKAVGDDDMLKSLQEVVQLQLFEMAQTSVFKLMSSDSVPKFLRDPKYSAI   685
SST2    ARYGMDNTQNDTKSVDSFPATLKVLRKLYPLFEIVSNEMYRLMNNDSFQKFTQSDVVYKD   687
consensus                                F  **  ** LM  *S **F     *
```

c

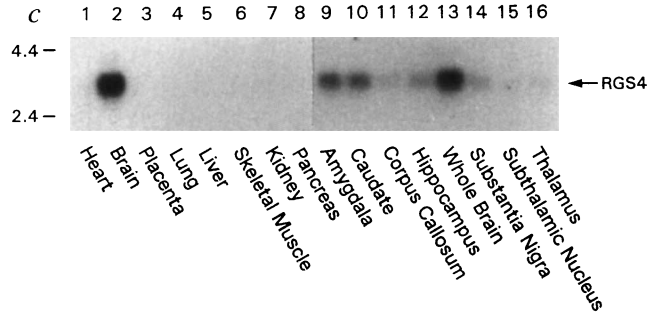

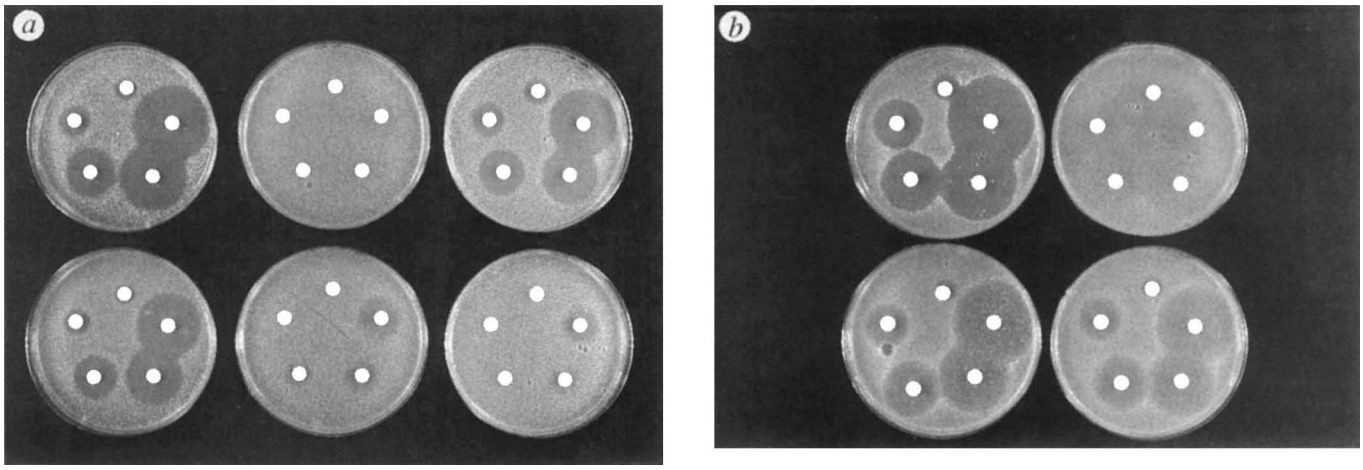

FIG. 3 Pheromone response in yeast cells expressing *RGS* family members. *a*, Pheromone response in an *sst2*Δ mutant. An *sst2*Δ mutant (AG57) was transformed with a control plasmid (pBM743) (top left), pVT102U–*RGS4* (top middle), pBM743–*RGS2* (top right), pBM743–*RGS3* (bottom left), pBM743–*RGS3T* (bottom middle), and pBM743–*RGS1* (bottom right). Equal numbers of cells (10^4) were plated in top agar on Sgal–ura plates. Amounts of pheromone (α-factor) applied to each disc increase anti-clockwise from the top of the disk (3, 10, 30, 100 and 300 pmol). Plates were incubated at 30 °C for 48 h and then photographed. Relative pheromone sensitivity is indicated by the size of the clear zone elicited in response to a given dose of pheromone. *b*, Pheromone response in cells expressing *SST2*. An *SST2*-expressing strain (AG56) was transformed with a control plasmid (pBM743) (top left), pVT102U–*RGS4* (top right), pBM743–*RGS3T* (bottom left), and pBM743–*RGS1* (bottom right). Halo assays were performed as above, except that the amounts of pheromone applied to discs (increasing anti-clockwise from the top) were 10, 30, 100, 300 and 1000 pmol. *c*, Effect of *RGS4* expression on pheromone-induced gene expression. An *sst2*Δ mutant (AG57) contained the *FUS1–lacZ* reporter plasmid pSL307 and either a control plasmid (pVT102U) (diamonds) or pVT102U–*RGS4* (squares). Cells were treated for 2 h at 30 °C with the indicated concentrations of α-factor, permeabilized, and assayed for expression of β-gal activity. Each curve is the average of assays performed in duplicate from three independent transformants.

METHODS. Assays of pheromone-induced growth arrest and gene expression have been described previously[26]. Yeast strains used were BC180 (*MAT***a** *leu2-3, 112 ura3-52 his3*Δ*1 ade2-1 sst2-*Δ*2*; obtained from J. Thorner), AG56 (*MAT***a** *leu2 ura3 his3 ade2 trp1 sst1*Δ); and AG57 (*MAT***a** *leu2 ura3 his3 ade2 trp1 sst2*Δ).

nor *SST2* overexpression attenuated the signal caused by overexpression of a constitutively active *STE11* (*STE11ΔN*), suggesting that they function upstream of the MAP kinase cassette (data not shown). To initiate signalling more proximally in the pathway, we used a strain lacking G-protein α-subunits that contains a temperature-sensitive *STE5* mutation[4,9]. In these cells, free G-protein βγ subunits transmit a constitutive signal that is reversibly blocked downstream by the temperature-sensitive mutation. After releasing the signal blockade, we observed no effect of either *RGS4* or *SST2* overexpression on signal transduction through the pathway. In the control cells, we detected 596 ± 50 Miller units of β-gal activity with the pheromone-inducible *lacZ* reporter plasmid pJD11, 6 h after shifting them to the permissive temperature. In those cells in which we overexpressed *SST2* or *RGS4*, we detected 662 ± 79 units and 608 ± 87 units of β-gal activity, respectively, after 6 h. These results demonstrate that *RGS4*, like *SST2* (refs 8–10), requires the G-protein α-subunit to function.

To verify that RGS family members inhibit MAP kinase activation in analogous pathways in mammalian cells, we first examined the activation of extracellular-signal-regulated kinase (ERK) 1 in response to interleukin (IL)-8. We used 293T cells permanently transfected with the IL-8 receptor, a seven-transmembrane helix-domain-containing receptor linked to a trimeric G protein[18,19]. IL-8 induced a 16-fold increase in ERK1 kinase activity, and the presence of *RGS1*, *RGS2*, *RGS3* and *RGS4* reduced the activity by a factor of 2, 1.6, 4, and 5.3, respectively (Fig. 4*a*). Increasing amounts of *RGS4* progressively inhibited IL-8-induced ERK1 kinase activity (data not shown). In contrast, *RGS3* failed to impair ERK1 activation by phorbol esters (Fig. 4*b*) or by an oncogenic, active Raf-1 (data not shown).

We next examined the role of an individual *RGS* family member in a native mammalian system. We took advantage of the known expression of RGS1 in activated B lymphocytes[12,13] and determined its effect on signalling through the platelet-activating factor (PAF) receptor, which is expressed on many B cell lines. PAF treatment activates MAP kinase and increases intracellular calcium levels by means of a heterotrimeric G protein(s)[20,21]. The

FIG. 4 Effect of *RGS* family members on MAP kinase activation in ▶ mammalian cells. *a*, RGS family members impair MAP kinase activation. 293T cells permanently transfected with the IL-8 receptor (6E cells) were transfected with a haemagglutinin (HA)-tagged *ERK1* construct in conjunction with empty vector or various *RGS* expression plasmids. Transfected cells were exposed to IL-8 for 3 min before immunoprecipitation of HA–ERK1 and assay of kinase activity. *b*, RGS3 fails to impair PMA-induced MAP kinase activation. 293T cells were transfected with the HA-tagged *ERK1* construct in conjunction with empty expression vector or *RGS3* expression vector. The cells were unstimulated (lane 1) or stimulated with PMA (50 ng ml^{-1}) for 20 min (lanes 2–4) before immunoprecipitation of HA–ERK1. The cells in lane 2 were exposed to pertussis toxin for the last 12 h of the culture period. *c*, *RGS1* expression inhibits PAF-induced increases in MAP kinase activity. Levels of RGS1 in *RGS1*-transfected HS-Sultan cell lines (3 separate cell lines labelled Tf7, Tf8 and Tf12) or a

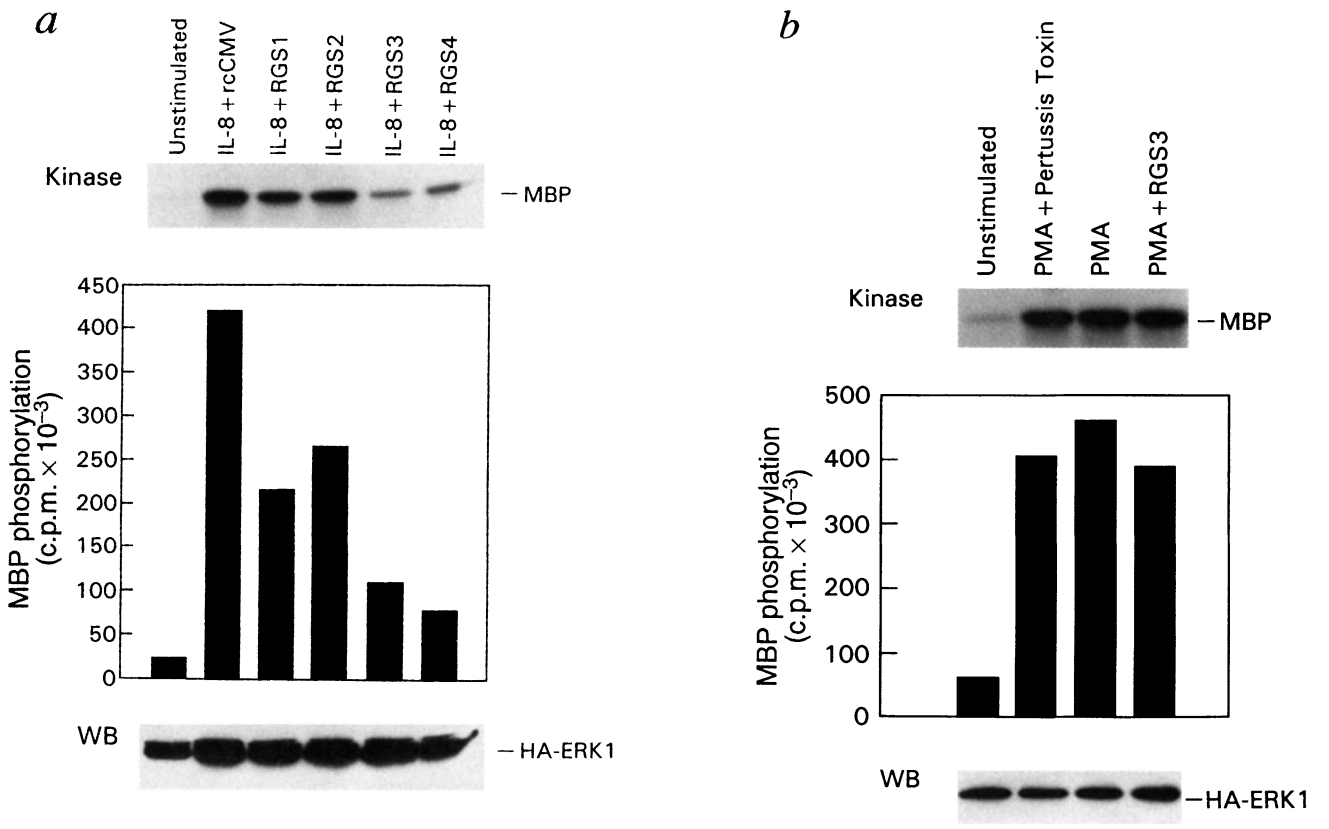

control cell line (vector) detected by immunoblotting (inset). The various cell lines were exposed to PAF (10^{-7} M) for 1 min and levels of MAP kinase activity measured in ERK2 immunoprecipitates. *d*, Induction of RGS1 following treatment with PAF and effect of transiently expressing *RGS1*. HS-Sultan cells were treated with PAF (10^{-7} M) or PMA (50 ng ml^{-1}) for 12 h and lysates immunoblotted with an RGS1 antiserum (left, lanes 1–3). ERK1 activity in HA-immunoprecipitates from HS-Sultan cells transiently transfected with *HA-ERK1* and vector control, *RGS1*, or antisense *RGS1*, and exposed to PAF for 1 min or not (right, bottom). Equivalent ERK1 levels were detected by HA-immunoblotting (right, top).

METHODS. For each experimental point in *a* and *b*, approximately 2×10^6 cells were transfected by a calcium phosphate method using 5 μg of a HA-tagged *ERK1* expression vector, *HA-ERK1* (provided by J. Kyriakis) in conjunction with 10 μg of the empty expression vector rcCMV, or one of the following *RGS* expression vectors: *RGS1*rcCMV, *RGS2*rcCMV, *RGS3*rcCMV or *RGS4*pCR3. After 36 h, the cells were collected, washed and exposed to recombinant human IL-8 (100 ng ml^{-1}) for 3 min at 37 °C. HA immunoprecipitations and kinase assays were performed as described previously[27]. The number of counts per minute in excised bands is indicated. The level of HA-ERK1 in the cell lysates was determined by immunoblotting with an anti-HA monoclonal antibody (labelled WB). HS-Sultan cells were obtained from the American Type Culture Collection and transfected with *RGS1* using the retroviral vector LXSN. Three pools of neomycin-resistant cells were assayed for RGS1 levels by immunoblotting with rabbit antisera raised against an RGS1 N-terminal peptide. A pool of vector-transfected cells served as the control cells. MAP kinase immunoprecipitations (10^7 cells per point) were performed as above, except the permanently *RGS1*-transfected cell lines where an ERK2-specific antiserum was used. Transient transfections of HS-Sultan cells with rcCMV, *AS-RGS1*rcCMV, *RGS1*rcCMV (5 μg) and *HA-ERK1* (5 μg) were performed by electroporation as described previously[28].

constitutive expression of RGS1 in HS-Sultan cells, a human B-cell lymphoma cell line that lacks significant levels of RGS1, markedly decreased PAF-induced MAP kinase activity (Fig. 4*c*). In addition, PAF induced RGS1 expression in HS-Sultan cells, and transient expression of RGS1 inhibited PAF-induced increases in MAP kinase activity (Fig. 4*d*). These results suggest that RGS1 participates in a negative feedback loop to decrease signal transduction through the PAF receptor.

These (and previous) results are consistent with models in which Sst2p and RGS4 (and presumably other RGSs) negatively regulate signalling upstream or at the level of the heterotrimeric G protein[6,10]. Furthermore, genetic studies in *C. elegans* indicate that an *RGS* family member, *egl-10*, negatively regulates signalling through GOA-1 (a homologue of the mammalian G_o proteins) at the level upstream of the G protein[22]. Although, under certain circumstances, *SST2* is required for the rapid degradation of the G-protein α-subunit[23], it is unlikely that regulating the stability of the α-subunit is the normal function of Sst2p or the RGS family members. The Sst2p-dependent degradation of the α-subunit occurred after overexpression of components of the ubiquitin-mediated protein degradation machinery[23]. However, in wild-type yeast, steady-state levels of the α-subunit are unaffected by *SST2* (ref. 10) and, similarly, in HS-Sultan cells the levels of α-subunits are unchanged by *RGS1* overexpression (data not shown). In addition, yeast that lack components of the ubiquitin-mediated protein degradation machinery are not supersensitive to pheromone[24], and *SST2* overexpression in these mutants promotes rapid recovery from pheromone-induced cell-cycle arrest (data not shown). Although further genetic and biochemical studies are needed to determine how *SST2* and *RGS*s inhibit G-protein-mediated MAP kinase activation, they probably regulate the function of G proteins directly, because Sst2p and Gpa1p associate *in vivo* and *in vitro* (H. Dohlman and J. Thorner, personal communication), and because a mammalian RGS family member has been shown to bind $G\alpha_{i3}$ (ref. 25).

It is likely that individual RGS family members preferentially regulate specific G proteins or G-protein-linked signalling pathways. The four characterized family members differed in their patterns of tissue expression and in their ability to impair IL-8 receptor signalling, providing some evidence of selectivity. Further specificity may be achieved by regulating their induction. As with *SST2*, *RGS* family members may be induced by signals generated through G-protein-linked receptors to trigger a desensitization mechanism. □

Received 31 October 1995; accepted 18 January 1996.

1. Sprague, G. F. Jr. & Thorner, J. in *Pheromone Response and Signal Transduction during the Mating Process of* Saccharomyces cerevisiae (eds Broach, J. R., Pringle, J. R. & Jones, E. W.) 657–744 (Cold Spring Harbor Laboratory Press, New York, 1992).
2. Kurjan, J. *A. Rev. genet.* **27,** 147–179 (1993).
3. Moore, S. A. *J. biol. Chem.* **259,** 1004–1010 (1984).
4. Chan, R. K. & Otte, C. A. *Molec. cell. Biol.* **2,** 11–20 (1982).
5. Chan, R. K. & Otte, C. A. *Molec. cell. Biol.* **2,** 21–29 (1982).
6. Dietzel, C. & Kurjan, J. *Molec. cell. Biol.* **7,** 4169–4177 (1987).
7. Steven, M., Betz, R. & Duntze, W. *Molec. gen. Genet.* **219,** 439–444 (1989).
8. Blinder, D. & Jenness, D. D. *Molec. cell. Biol.* **9,** 3720–3726 (1989).
9. Hasson, M. S., Blinder, D., Thorner, J. & Jenness, D. D. *Molec. cell. Biol.* **14,** 1054–1065 (1994).
10. Dohlman, H. G. *et al. Molec. cell. Biol.* **15,** 3635–3643 (1995).
11. Adams, T. H., Hide, W. A., Yager, L. N. & Lee, B. N. *Molec. cell. Biol.* **12,** 3827–3833 (1992).
12. Hong, J. X., Wilson, G. L., Fox, C. H. & Kehrl, J. H. *J. Immun.* **150,** 2895–3904 (1993).
13. Newton, J. S. *et al. Biochem. biophys. Acta* **1216,** 314–316 (1993).
14. Siderovski, D. P., Heximer, S. P. & Forsdyke, D. R. *DNA Cell Biol.* **12,** 125 (1994).
15. Wilson, R. *et al. Nature* **368,** 32–38 (1994).
16. Lupas, A., Van Dyke, M. & Stock, J. *Science* **252,** 1162–1164 (1991).
17. Cairns, B. R., Ramer, S. L. & Kornberg, R. D. *Genes Dev.* **6,** 1305–1318 (1992).
18. Murphy, P. M. & Tiffany, H. L. *Science* **253,** 1280–1283 (1991).
19. Van Lint, J. *et al. Molec. cell. Biochem.* **127,** 171–177 (1993).
20. Mazer, B. D., Sawami, H., Todai, A. & Gelfand, E. W. *J. clin. Invest.* **90,** 759–765 (1993).
21. Franklin, R. A. *et al. J. Immun.* **151,** 1802–1810 (1993).
22. Koelle, M. R. & Horvitz, H. R. *Cell* **84,** 115–125 (1996).
23. Madura, K. & Varshavsky, A. *Science* **265,** 1454–1458 (1994).
24. Dohmen, R. J., Madura, K., Bartel, B. & Varshavsky, A. *Proc. natn. Acad. Sci. U.S.A.* **88,** 7351–7355 (1991).
25. De Vries, L. *et al. Proc. natn. Acad. Sci. U.S.A.* **92,** 11916–11920 (1995).
26. Weiner, J. L., Guttierez-Steil, C. & Blumer, K. J. *J. biol. Chem.* **268,** 8070–8077 (1993).
27. Kyriakis, J. M. *et al. Nature* **369,** 156–160 (1994).
28. Thevenin, C., Lucas, B. P., Kozlow, E. J. & Kehrl, J. H. *J. biol. Chem.* **268,** 5949–5956 (1993).

ACKNOWLEDGEMENTS. K.M.D., K.J.B and V.H.K. contributed equally to this work. We thank K. Harrison, G. L. Wilson and M. Downs for technical assistance; M. Rust for editorial assistance; B. Cairns, D. Jenness, J. Thorner and D. Tipper for yeast strains and plasmids; P. De Camilli for the rat brain cDNA expression library; S. Ahuja for the IL-8 receptor-transfected 293T cells; and A. S. Fauci for support. This work was supported in part by grants from the NIH and the American Heart Association (K.B.). The accession numbers for the sequences reported here are U27655 (*RGS3*), U27767 (rat *RGS4*) and U27768 (human *RGS4*).

RNA binding and translational suppression by bicoid

Rolando Rivera-Pomar*, Dierk Niessing*, Urs Schmidt-Ott*, Walter J. Gehring† & Herbert Jäckle*

* Abteilung Molekulare Entwicklungsbiologie, Max-Planck-Institut für biophysikalische Chemie, Am Fassberg, D-37077 Göttingen, Germany
† Biozentrum der Universität Basel, Klingelbergstrasse 70, CH-4056 Basel, Switzerland

THE anterior determinant bicoid (bcd) of *Drosophila* is a homeodomain protein. It forms an anterior-to-posterior gradient in the embryo and activates, in a concentration-dependent manner, several zygotic segmentation genes during blastoderm formation[1–4]. Its posterior counterpart, the homeodomain transcription factor caudal (cad)[5–7], forms a concentration gradient in the opposite direction, emanating from evenly distributed messenger RNA in the egg. In embryos lacking bcd activity as a result of mutation, the cad gradient fails to form and cad becomes evenly distributed throughout the embryo[8]. This suggests that bcd may act in the region-specific control of *cad* mRNA translation. Here we report that bcd binds through its homeodomain to *cad* mRNA *in vitro*, and exerts translational control through a bcd-binding region of *cad* mRNA.

Maternal *cad* mRNA is evenly distributed in the early cleavage-stage embryo (Fig. 1*a*), and cad forms a posterior-to-anterior concentration gradient before the initiation of zygotic gene expression[6,7] (Fig. 1*b*, *d*). In the absence of functional *bcd* expression (Fig. 1*c*, *d*), cad remains evenly distributed in the embryos[8] (Fig. 1*e–g*). To see whether *cad* mRNA may represent a direct target of *bcd*, we performed crosslinking and filter-binding experiments involving nuclear extracts from *Drosophila* embryos and bacterially expressed bcd.

Crosslinking experiments indicated specific binding of labelled *cad* mRNA (Fig. 2*a*) to three different proteins, p125 and the protein doublet p83/p71, present in nuclear extracts from wild-type embryos (Fig. 2*b*). The p83/p71 doublet could be immunoprecipitated with anti-bcd antibodies (Fig. 2*b*): *cad* mRNA binding was also seen in crosslinks with recombinant bcd (not shown). However, the p83/p71 doublet was absent from nuclear extracts of embryos obtained from bcd mutant females (Fig. 2*b*) and from bcd-depleted nuclear extracts of wild-type embryos (data not shown). The p125 protein was found in both cases binding to the region 1,916–2,028, which overlaps the maternal and zygotic polyadenylation signals (Fig. 2*d*). Thus the p83/p71 doublet, which binds to *cad* mRNA *in vitro*, is bcd.

The binding of bcd occurs within a 120-nucleotide region of *cad* mRNA (position 1,350–1,470; see Fig. 2*a*; position 1 is the first nucleotide of the start codon[9]), which extends into the 3′ untranslated region (Fig. 2*c*). The *bcd* protein did not bind to other regions of *cad* mRNA, nor did it bind to *cad* mRNA of the lower dipteran species *Clogmia albipunctata* (U.S.-O., unpublished results) which is thought to lack bcd as an anterior morphogen. We refer to the bcd-binding sequence interval 1,350–1,470 of *cad* mRNA in *Drosophila* as the bcd binding region (BBR).

To identify the RNA-binding domain of bcd, we performed filter-binding assays using truncated forms of bcd. The results summarized in Fig. 2*e* indicate that truncated bcd containing the